Electronic structure and magnetism of ferromagnetic GdTiSi and GdTiGe

2001 J. Phys.: Condens. Matter 13 6397

(http://iopscience.iop.org/0953-8984/13/29/309)

INSTITUTE OF PHYSICS PUBLISHING JOURNAL OF PHYSICS: CONDENSED MATTER

J. Phys.: Condens. Matter **13** (2001) 6397–6409 PII: S0953-8984(01)22499-0

Electronic structure and magnetism of ferromagnetic GdTiSi and GdTiGe

G Skorek[1], J Deniszczyk[1,2], J Szade[1] and B Tyszka[1]

[1] A Chelkowski Institute of Physics, University of Silesia, Uniwersytecka 4, 40-007 Katowice, Poland
[2] Institute of Physics and Chemistry of Metals, University of Silesia, Uniwersytecka 4, 40-007 Katowice, Poland

Received 5 March 2001
Published 6 July 2001
Online at stacks.iop.org/JPhysCM/13/6397

Abstract

Crystal structure and temperature dependence of magnetic susceptibility and electrical resistivity have been determined for GdTiSi and GdTiGe. Both compounds order ferromagnetically and for GdTiGe T_C is 374 K which is a very high value for such kinds of compounds. The electronic structure for both compounds has been investigated by photoelectron spectroscopy and compared with calculations performed using the TB-LMTO method. A very good agreement with experiment was obtained, especially for GdTiGe. A strong hybrydization between the d states from Gd and Ti was found and a significant polarization of the Ti 3d electrons in GdTiGe was obtained which may be related to the enhanced indirect exchange between Gd magnetic moments.

1. Introduction

Magnetic and crystallographic properties of rare-earth ternary intermetallic compounds has been the subject of intensive research. The large group of RTX compounds, where R is a rare-earth element, T is a transition-3d element and X is a p-electron metal, is particularly interesting. Only a few compounds have been found where T is Ti and X is Ge or Si. Very recently a systematic crystallographic study of RTiGe has been performed and the tetragonal CeScSi structure type (space group I4/mmm) was found [1, 2]. Morozkin *et al* reported on ferromagnetism in GdTiGe with a high $T_C = 376$ K [2]. The former results obtained on GdTiGe were contradictory as regards the crystal structure and magnetism [3, 4]. Nikitin *et al* reported antiferromagnetic ordering at a relatively high temperature: $T_N = 412$ K with a positive paramagnetic Curie temperature $\theta_p = 317$ K and a structure of CeFeSi type (space group P4/nmm) [3]. However, Welter *et al* found a ferromagnetic order below 400 K, where the crystal structure was of La_2Sb type [4]. On the other hand, Morozkin [5] concluded that GdTiGe exists in two phases: a high-temperature modification of CeFeSi type and a low-temperature modification of CeScSi structure type.

Also for GdTiSi, various types of crystal structure have been reported. Kido *et al* described the hexagonal AlB_2 type of crystal structure (space group P/6mmm) and found a paramagnetic behaviour down to 77 K [6]. Recently Morozkin [7] reported that GdTiSi crystallizes in the tetragonal CeFeSi-type structure (space group P4/nmm, $a = 0.4027(1)$ nm, $c = 0.7553$ nm). For this type of structure no magnetic data were available. For some GdTSi and GdTGe compounds, where T is a transition metal, the effect of substitution for Ti has been investigated with respect to crystallographic and magnetic properties [2, 8].

The aim of this paper is to perform the complex investigation of GdTiSi and GdTiGe ternary compounds including their electronic structure. Both theoretical calculations, using the LMTO method, and the experimental electronic structure, have been determined. X-ray photoemission spectroscopy (XPS) and ultraviolet photoemission spectroscopy (UPS) were used. The model spectra of valence bands based on the calculations are compared with the experimental ones. The crystal structure has been refined using the Rietveld method. Moreover, the DC and AC magnetic susceptibility and electrical resistivity have been measured as functions of temperature.

The origin of the high magnetic ordering temperatures and the role of the polarization of Ti 3d and Gd 5d electrons in indirect exchange interactions are discussed.

2. Experimental

Samples of GdTiSi and GdTiGe were obtained by the Czochralski method from a levitated melt using gadolinium of 99.9% purity, titanium 99.99%, silicon and germanium 99.999%. The temperature during the crystal growth was about 2000 K. The cylindrical samples were polycrystalline or consisted of large grains. The samples of GdTiSi were annealed at 750°C for two days. The structure of the compounds was identified by x-ray powder diffraction with Cu Kα radiation using a Siemens D-5000 diffractometer. The Rietveld refinement of the structure was performed using the FullProf program. In addition, the atomic composition of the samples was checked using x-ray photoelectron spectroscopy (XPS) and Auger electron spectroscopy (AES). Magnetic susceptibility measurements were performed using the Faraday method, in the temperature range 77–800 K under an atmosphere of helium. The AC magnetic susceptibility was measured in the temperature range 4.2–300 K, at a frequency of 700 Hz. The electrical resistivity was measured using the van der Pauw method in the temperature range 4.2–300 K. Measurements were made throughout the complete cooling–heating cycles. The XPS measurements were performed with a Physical Electronics PHI 5700/660 spectrometer, using monochromatized Al Kα radiation (1486.6 eV). The vacuum during the measurements was about 10^{-10} Torr. The energy resolution was about 0.35 eV. The UPS spectra were obtained using a helium lamp emitting radiation of 21.2 eV (He I) and 40.8 eV (He II). The samples were fractured or scraped with a diamond file in the UHV chamber just before acquiring the spectra. For some of them, sputtering with low-energy Ar ions was used to ensure the surface was free from contaminants.

Band-structure calculations were carried out with the use of the tight-binding linear muffin-tin orbital (TB-LMTO) method of Andersen *et al* [9]. The calculations were scalar relativistic, without the spin–orbit interaction. The exchange-correlation (XC) potential was taken within the local spin-density approximation (LSDA), with the use of the von Barth–Hedin [10] parametrization, the explicit form of which was cited in e.g. [11]. The non-local correction to the XC potential was taken into account within the Langreth–Mehl–Hu (LMH) gradient approximation [12]. In the TB-LMTO method the crystal potential is treated within the atomic-sphere approximation (ASA) and the crystal volume is divided into overlapping Wigner–Seitz (WS) spheres of radius r_s^i. To reduce the effect of overlapping spheres the

standard combined correction [9] was used in the calculations. The ASA demands that the volume equation be obeyed. If by $r_s^{\mathrm{av}} = (\sqrt[3]{3V/4\pi n_{\mathrm{at}}})$ we denote the average WS radius then the volume equation reads $\sum_{i=1}^{n_{\mathrm{at}}}(w_i)^3 = n_{\mathrm{at}}$, where n_{at} is the number of atoms in the unit cell and $w_i = r_s^i/r_s^{\mathrm{av}}$. In the calculations the w_i ratios were chosen so as to minimize overlap of the spheres and to have close values of the atomic potential at the sphere boundaries of different atoms in the unit cell. The ratios were: $w_{\mathrm{Gd}} = 1.08$, $w_{\mathrm{Ti}} = 0.98$, $w_{\mathrm{Ge}} = 0.92$ in GdTiGe and $w_{\mathrm{Gd}} = 1.07$, $w_{\mathrm{Ti}} = 0.98$, $w_{\mathrm{Si}} = 0.94$ in GdTiSi. Self-consistent calculations were performed for more then 200 *k*-points in the irreducible part of the Brillouin zone (IBZ). For the purposes of the DOS plotting and the calculations of the XPS and UPS spectra, additional iterations with more then 1000 *k*-points in the IBZ were performed.

3. Results and discussion

3.1. Crystal structure

The analysis of the powder x-ray diffractograms show that GdTiSi crystallizes in a tetragonal CeFeSi type of structure (P4/nmm), whereas GdTiGe crystallizes in a tetragonal CeScSi type (I4/mmm). The lattice parameters of GdTiGe determined at room temperature and the fractional positional coordinates parameters are given in table 1. For GdTiGe the type of crystal structure is in agreement with the recent data of Welter *et al* [1]; the *a* lattice constant obtained from our analysis is slightly larger but the *c* one is smaller. The fractional coordinates of atoms are similar, excluding the *x* position of the Ti 4(c), which was reported in [1] as being 0.5. Our data indicate that parameter to be equal to 0, which is, on the other hand, in agreement with Morozkin [5].

Table 1. Lattice parameters and atomic position parameters of the GdTi(Si, Ge) ternary compounds.

Compound	*a* (nm)	*c* (nm)	Type position	*x*	*y*	*z*
GdTiSi	0.4046(2)	0.7625(6)	Gd 2(c)	0.250	0.250	0.655
			Ti 2(a)	0.750	0.250	0.000
			Si 2(c)	0.250	0.250	0.258
GdTiGe	0.4079(1)	1.545(5)	Gd 4(e)	0.000	0.000	0.327
			Ti 4(c)	0.000	0.500	0.000
			Ge 4(e)	0.000	0.000	0.122

For GdTiSi the lattice parameters and the fractional positional coordinate parameters are in fair agreement with the published data of Morozkin [7] (table 1). The sample was contaminated by a small amount of Ti_5Si_3, which does not influence, in our opinion, the magnetic and electronic properties of GdTiSi.

3.2. Magnetic properties

Figure 1 shows the temperature dependence of the DC magnetic susceptibility and its reciprocal for GdTiSi and GdTiGe in the temperature range 77.7–800 K. Complete cooling–heating cycles were performed for both compounds. GdTiSi exhibits a ferromagnetic transition at about 294 K which is followed by an increase in magnetization when temperature decreases down to 200 K . The AC magnetic susceptibility shows a gradual increase of susceptibility between 291 and 200 K, indicating that the transition is not a simple ferromagnetic one (figure 2). The effective moment per Gd atom, derived from temperatures above 450 K, is 7.47 μ_{B};

the paramagnetic Curie temperature θ_p is 299 K, which is very close to T_C. In GdTiGe the ferromagnetic transition is visible at about 374 K and the molar magnetization below T_C is much larger than for GdTiSi (figure 1). The Curie–Weiss law is obeyed only above 650 K and the parameters derived for $T > 650$ K are $\mu_{eff} = 7.81\ \mu_B$ and $\theta_p = 433$ K (see table 2). Below that temperature the inverse susceptibility exhibits a curvature which is often encountered in ferromagnetic Gd compounds [13, 14]. The AC magnetic susceptibility of GdTiGe shows a broad maximum below the ferromagnetic transition.

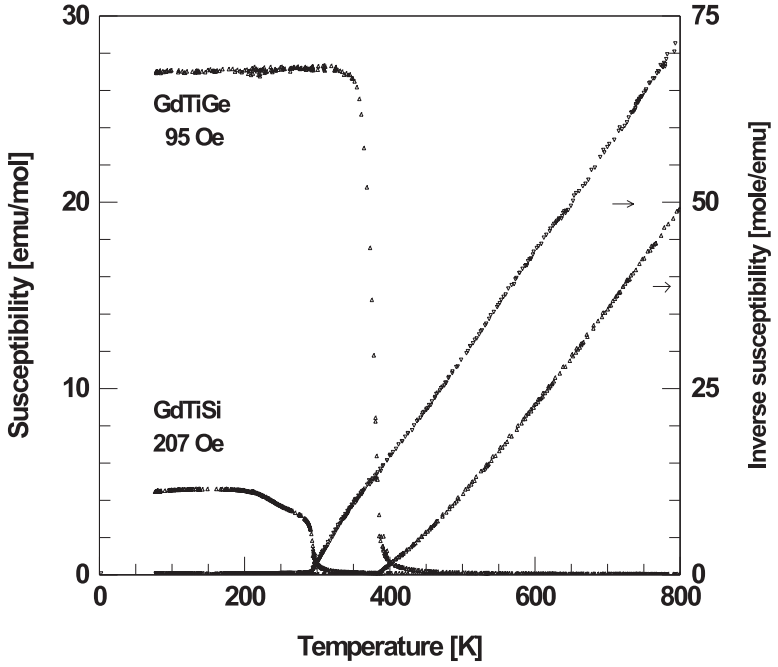

Figure 1. Temperature dependence of the DC magnetic susceptibility and reciprocal DC magnetic susceptibility of the GdTiSi and GdTiGe compounds.

Table 2. Magnetic ordering temperature T_C, paramagnetic Curie temperatures θ_p, and effective magnetic moments μ_{eff} per gadolinium atom of GdTiSi and GdTiGe compounds.

Compound	T_C (K) χ_{DC}	θ_p (K)	μ_{eff}/Gd (μ_B)	T_C (K) χ_{AC}
GdTiSi	294	299 for $T > 450$ K	7.47 for $T > 450$ K	291
GdTiGe	374	433 for $T > 650$ K	7.81 for $T > 650$ K	364

3.3. Electrical resistivity

The electrical resistivity for both compounds was measured mainly in the ferromagnetic state. For GdTiSi the transition at 290 K is only slightly pronounced (figure 3). ρ(T) shows a negative curvature for this compound in the large temperature range 40–290 K. The value of the residual resistivity ρ_0 for GdTiSi is 0.13 $\mu\Omega$ m at 4.2 K whereas for GdTiGe it is 0.66 $\mu\Omega$ m. The sample of GdTiGe consisted of relatively large crystals and was brittle, so the presence of possible microcracks at the grain boundaries may be the reason for the larger residual resistivity.

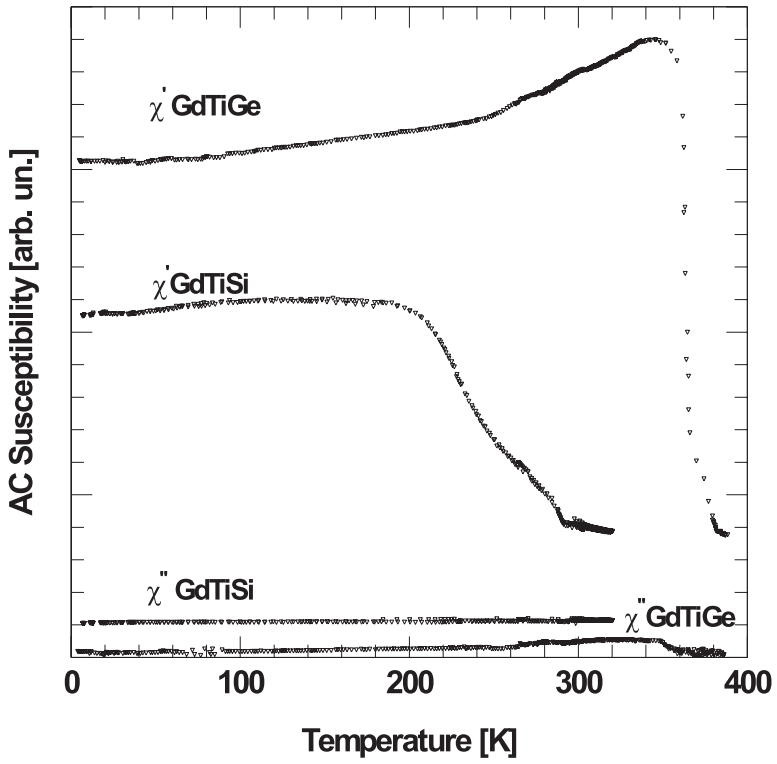

Figure 2. Temperature dependence of the AC magnetic susceptibility of the GdTiSi and GdTiGe compounds.

3.4. Electronic structure

The photoemission spectra from the valence bands of both compounds are shown in figure 4 in comparison with pure elements—gadolinium, germanium, silicon and titanium. The intensity of the spectra of Gd, GdTiSi and GdTiGe were normalized with respect to the Gd 4f photoemission intensity. Both compounds exhibited a similar shape of the valence band photoemission, which is quite different from the energy distribution curves (EDC) of the pure elements. The characteristic peak with a maximum at a binding energy of about 2 eV and a slightly pronounced feature close to the Fermi level were found earlier in other Gd compounds with Si or Ge [14, 15].

The UPS valence band of GdTiSi and GdTiGe, compared with pure Gd and Ti, are shown in figure 5. The characteristic feature of these spectra is a much more pronounced intensity at the binding energy just below the Fermi level.

The results of electronic structure calculations are shown in figures 6–9. From figure 6 it can be seen that the band structure of both compounds consists of a low-lying s-band of non-metal component X (=Si, Ge) separated by an energy gap of width 2.5 eV from the complex of the hybridized pd-bands of all (Gd, Ti and X) atoms. The complex of the pd-bands in GdTiGe is slightly narrower and much less hybridized than that in the GdTiSi compound. The calculated positions of the 4f-↑ band of the Gd atom differ significantly from the measured ones, which is a common feature of electronic structure calculations based on the standard LSDA type of XC potential even with gradient corrections. Too small binding

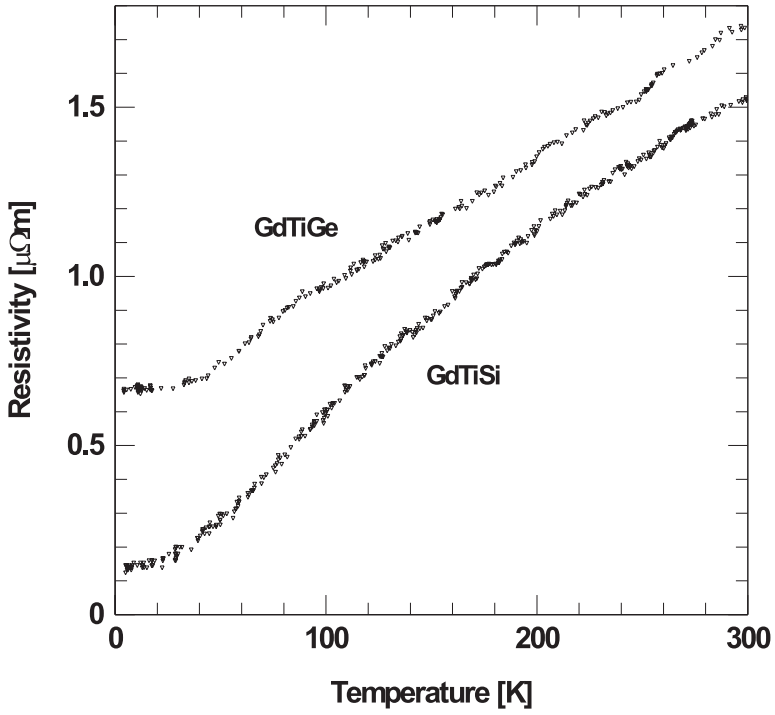

Figure 3. Temperature dependence of the electrical resistivity of the GdTiSi and GdTiGe compounds.

energy, and in effect a relatively high non-physical contribution to the total density of states at the Fermi level coming from the 4f-↓ states of the Gd atoms, is a consequence of the highly non-homogeneous 4f electron charge density and modelling nature of the LSDA.

In the last decade, two approaches improving the treatment of strongly correlated electronic band states, characterized by a non-homogeneous charge density distribution in the unit cell, have been proposed. The first, called the LDA + U approach, was developed by Anisimov *et al* [16]. This approach modifies the LSD XC-potential by the use of additional terms describing the correlation and exchange interaction within the narrow bands (d or f) calculated from the Hubbard Hamiltonian treated within the molecular field approach. The magnitudes of the exchange and correlation interactions of 4f-shell electrons are the free parameters of the method. Another approach that improves the LSDA, and gives a valid description of the physics of systems with narrow-band, strongly correlated electrons (d- and f-systems), introduces the self-interaction correction (SIC) to the LSD XC total energy functional [17]. In exact spin density functional theory (SDFT) the energy functional does not contain any self-energy interactions (SI). Also, in some approximated energy functionals (e.g. Hartree–Fock), the SI terms cancel out. The local approximation to the XC-potential leaves the SI terms in the energy functional not cancelled, and results in an erroneous physical description, especially of f-systems. The SIC-LSD approach consists of the augmentation of the LSD energy functional with terms that cancel the remaining SI contribution. Details of the SIC-LSD formalism, a description of its application to the LMTO band structure method and discussion of selected results can be found in [18] and references cited therein. Both the LDA + U and SIC-LSD are one-electron theories and work well for strongly correlated bands

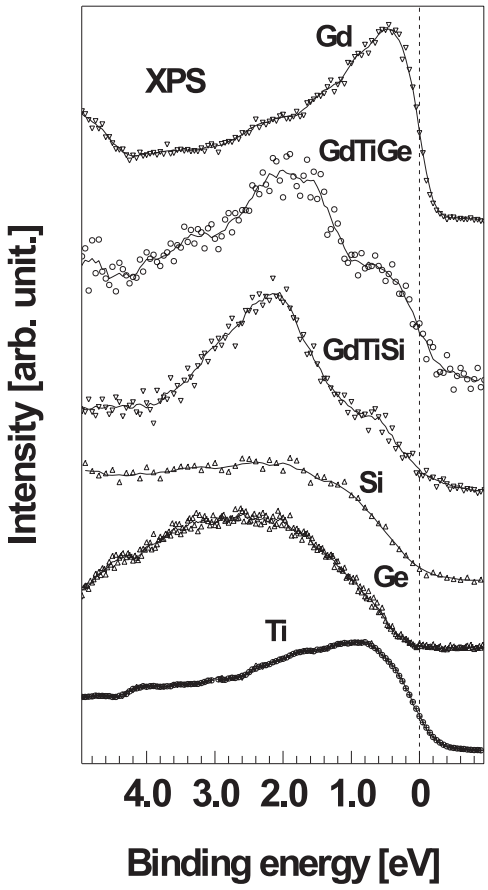

Figure 4. Valence band XPS spectra for the GdTiSi and GdTiGe compounds and pure elements Gd, Ge, Si, Ti.

where the $U/t \gg 1$ condition is satisfied (U and t are the Coulomb correlation and hopping integrals, respectively).

Surprisingly, despite the wrongly calculated energetic position of the 4f-↑ band for both compounds within the gradient-corrected LSDA approach, the shift of its location upon a change of chemical composition (GdTiSi → GdTiGe) is comparable with that observed experimentally (figure 6 and table 4 below). This may indicate that the effect of chemical shift of some energy levels (observed in Gd compounds) is not a local, atomic origin but results from the difference in electronic charge distribution within the unit cells of different chemical compositions.

Figures 7 and 8 collect the different contributions to the density of states (DOS) of the compounds and in table 3 values of the total and partial contributions to the DOS at the Fermi energy (ε_F) are given. Figure 9 shows simulated XPS and UPS spectra of GdTiX. The underlying data for XPS and UPS figures were prepared by convolution of the calculated partial DOS contributions by Lorentzians (with a half-width of 0.35 eV for XPS and 0.2 eV for UPS) and then multiplication by the corresponding cross sections taken from [19]. Analysis of the partial densities of states shown in figures 7 and 8 leads to the following observations. In both compounds the density of states near ε_F is dominated by the d-states of Ti atoms. In

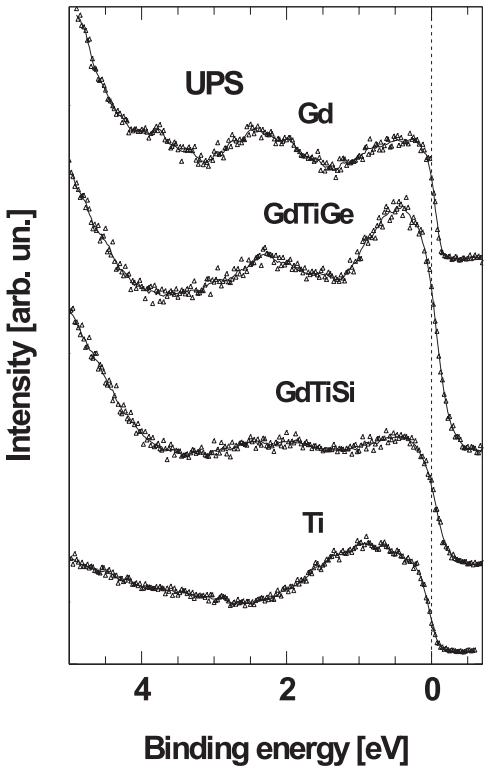

Figure 5. Valence band UPS spectra for the GdTiSi and GdTiGe compounds and pure element Ti.

Table 3. Partial atomic occupations n, magnetic moments μ (μ_B/atom) and density of states at Fermi energy $D(\varepsilon_F)$ (eV/atom), with separated orbital contributions (s + p, d and f). Values of the total magnetic moment (μ_{tot}) and the total DOS ($D_{tot}(\varepsilon_F)$) are given per formula unit.

	Gd	GdTiGe			GdTiSi		
	hcp	Gd	Ti	Ge	Gd	Ti	Si
n_{s+p}	1.26	1.07	1.37	3.83	1.08	1.35	3.88
n_d	1.61	1.7	2.58	0.17	1.65	2.56	0.23
n_f	7.13	7.14	—	—	7.13	—	—
μ_{s+p}	0.25	0.08	0.07	−0.03	0.04	0.00	−0.01
μ_d	0.42	0.38	0.61	0.05	0.25	−0.25	0.02
μ_f	6.88	6.86	—	—	6.87	—	—
μ_{tot} (μ_B/fu)	7.55		8.02			6.90	
$D_{s+p}(\varepsilon_F)$	0.38	0.19	0.35	0.26	0.08	0.21	0.24
$D_d(\varepsilon_F)$	1.29	1.19	2.38	0.19	0.53	1.36	0.14
$D_f(\varepsilon_F)$	0.56	0.31	—	—	0.14	—	—
$D_{tot}(\varepsilon_F)$ (eV/fu)	2.23		4.87			2.81	

the GdTiGe the Gd-5d states at ε_F are more strongly hybridized with Ti-3d states. The feature of the DOS located at the energy range from −4 to −2.5 eV is built by the s and p states of all atoms. Above this region up to −1 eV a sharp feature develops from hybridized p-states of

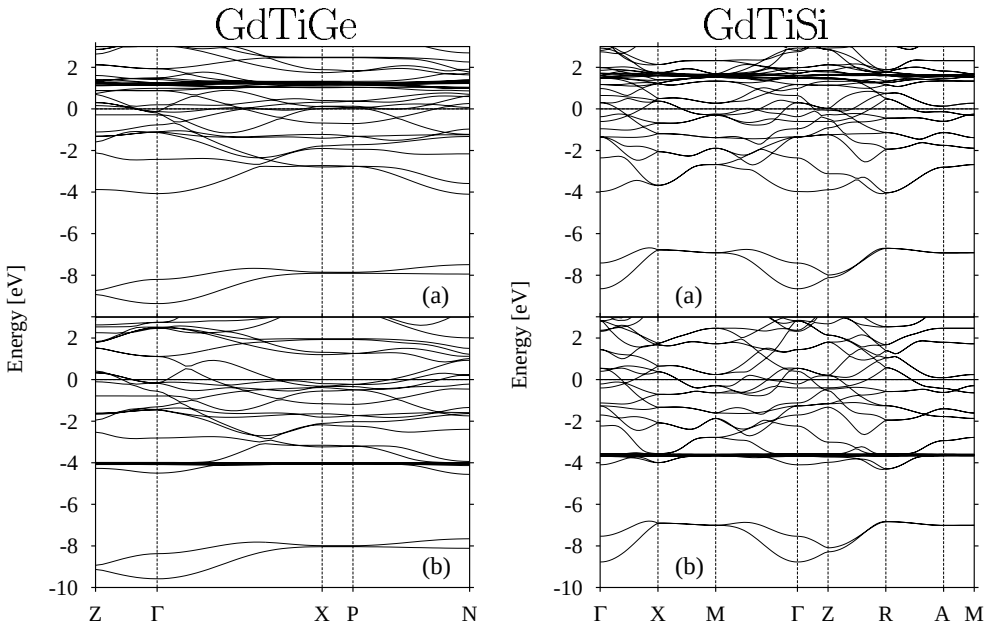

Figure 6. Minority (*a*) and majority (*b*) spin-energy bands of the GdTiGe and GdTiSi compounds.

the X atom with d-states of Gd and Ti. The calculations indicate that the main component in the energy region just below the Fermi level is due to the Ti 3d band. The simulated spectra of XPS differ quantitatively from those obtained for the UPS. The photoionization cross section for these electronic states is known to increase considerably at low photon energy of He II radiation in relation to other components [19]. This leads to a large difference in the shape of valence band spectra obtained at various photon energies. It is, however, worth noting that the calculation of cross sections are performed using atomic orbitals and the orbital character of various states in the valence band is preserved only partly. From analysis of the partial atomic contributions to the calculated XPS and UPS spectra it can be concluded that in both compounds the slight feature seen just below ε_F is built by hybridized d-states of Gd and Ti. The peak seen experimentally at a binding energy of $\sim$2 eV is built by the p-states of X atoms hybridized with 5d-states of Gd. In the UPS spectra of both compounds the whole spectrum is dominated by states of titanium. The Gd-states contribute much less while the Ge contribution is only slightly visible. Hybridization of rare-earth 5d electrons and 3d electrons from the transition metal was used to elucidate the magnetic properties of RT_2 compounds [20]. For GdTiGe a clear exchange splitting of both Gd and Ti d bands is visible (Figure 7).

For both compounds the simulated UPS and XPS spectra are shifted towards lower binding energy. For example the feature of XPS and UPS spectra observed experimentally at $\sim$2 eV on the simulated spectra is shifted to lower binding energy by some tenths of an eV. It appears that the shift of the whole spectra is caused by the presence of the 4f-$\uparrow$ band located erroneously in the close energy region. The level repulsion of the 4f-$\uparrow$ band with the pd-$\uparrow$ bands, which results from the hybridization interaction between the bands, could produce the shift of pd-band complex to lower binding energies.

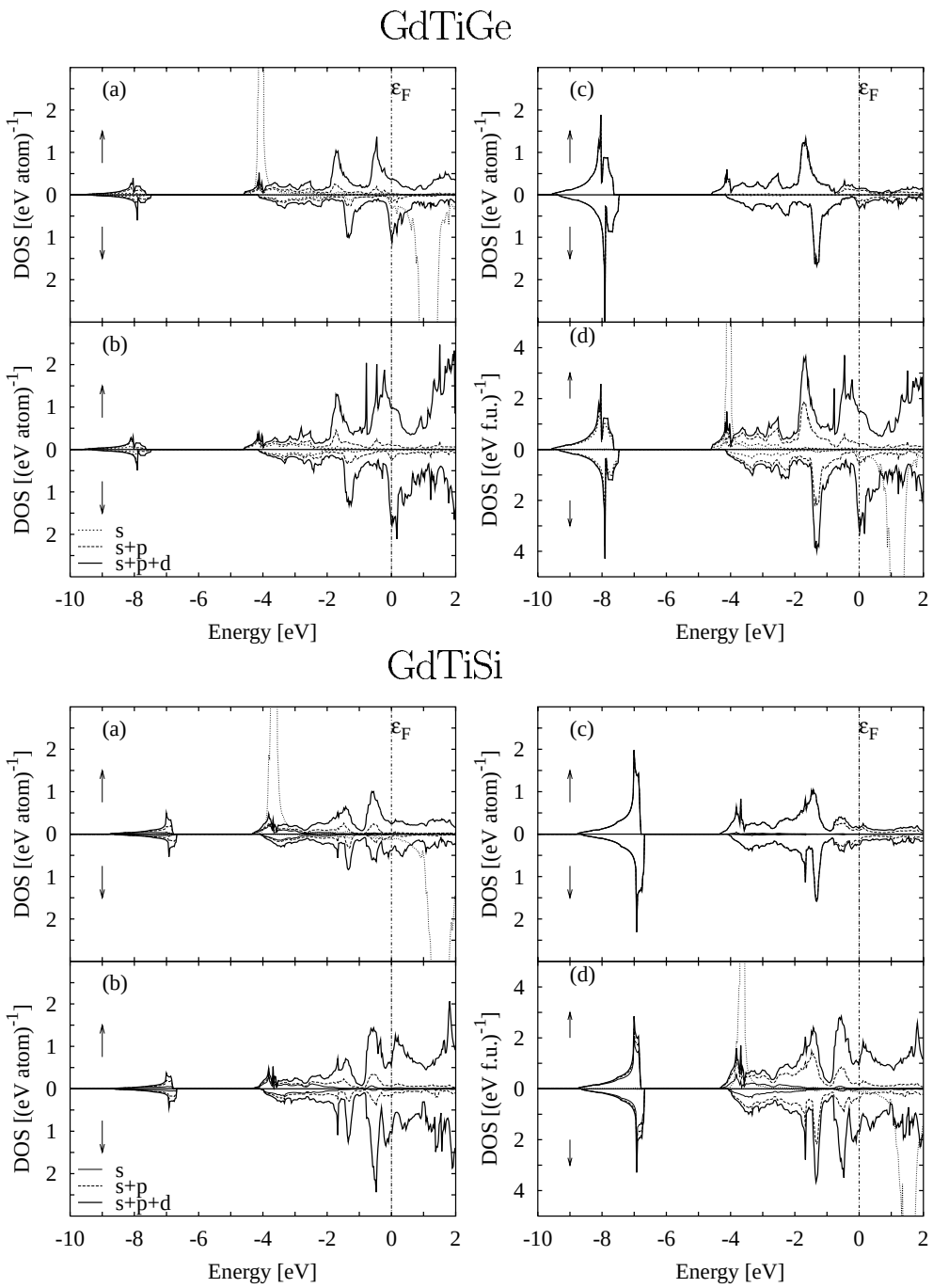

Figure 7. Spin-resolved, partial atomic (Gd (*a*), Ti (*b*) and Ge, Si (*c*)) and the total per formula unit (*d*) density of states for GdTi(Ge, Si) decomposed into s-, p- and d-type state contributions. The common to all parts, is given in (*b*). The Gd 4f-state DOS are represented by the dot line, and the dash-dotted line shows the position of the Fermi energy ε_F. (Note the different scale used in (*d*).)

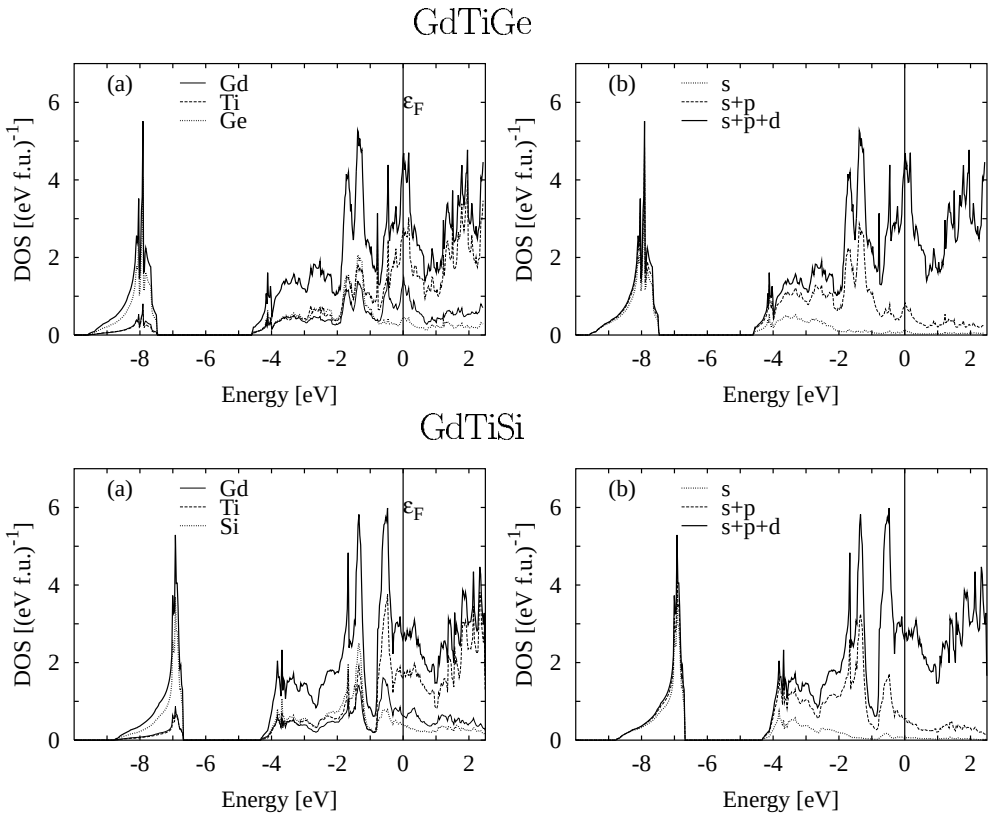

Figure 8. Total s + p + d DOS (thick solid line) of GdTiX (X = Ge, Si) with separated atomic contributions (*a*) and decomposed into s, p and d contributions (*b*). The Gd-4f states are not presented here. The vertical solid line shows the position of the Fermi energy ε_F.

Table 3 summarizes the calculated magnetic properties of the compounds. For the purposes of comparison the results for hcp-Gd calculated within the same framework are presented. The overall tendency observed experimentally is reproduced quite well. The effective magnetic moment per Gd atom for GdTiGe is larger by more than 1 μ_B than that for GdTiSi and larger by 0.45 than in the elemental hcp-Gd. Though the 4f-state contribution to the local magnetic moments of Gd atoms does not depend on the chemical environment, the total atomic magnetic moments of Gd atoms in both compounds are smaller than in hcp-Gd (7.3 and 7.2 μ_B in GdTiGe and GdTiSi, respectively). The reduction of the local Gd moment is a result of the differences in the magnetic polarization of the 5d-states of the Gd atom. On the other hand, the enhancement of the effective magnetic moment in GdTiGe is due to the polarization of the d-states on the Ti atom, which results in the effective d-band polarization in GdTiGe of the order of 1 μ_B (larger by 0.5 μ_B than that in hcp-Gd). Calculations for GdTiSi have shown that the observed reduction of effective magnetic moment is caused by the antiferromagnetic alignment of local d-band magnetic moments of the Gd and Ti atoms. As a result, the d-band contribution to the effective magnetic moment of GdTiSi disappears. The moments are calculated in the ferromagnetic state. It seems that the induced moment disappears above T_C as the effective moment derived from high temperatures is even lower for GdTiGe than that from the local 4f momentum (7.94 μ_B).

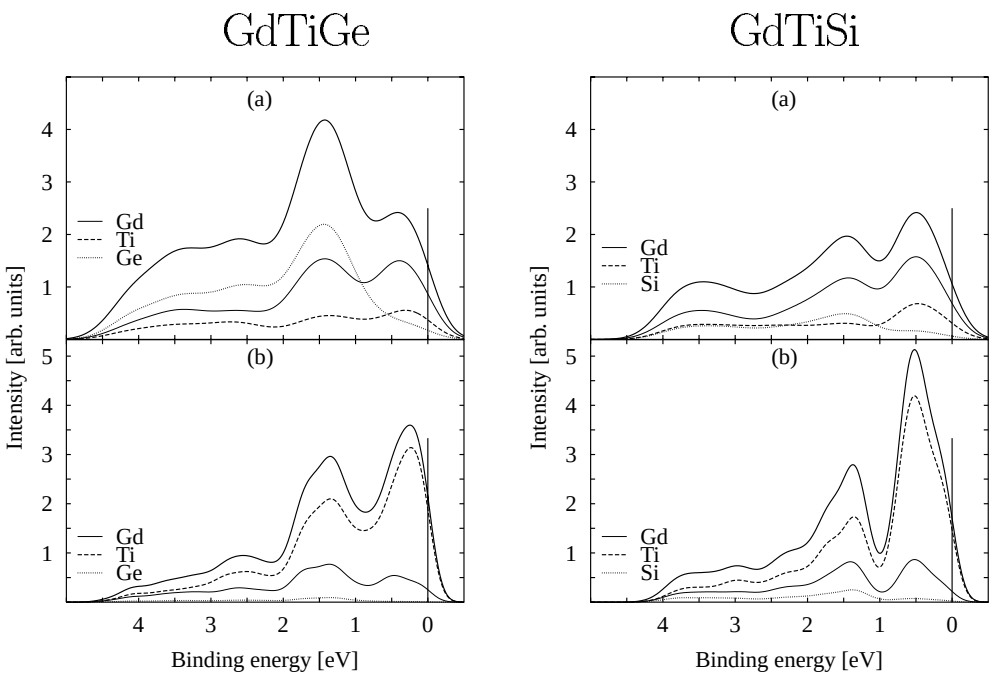

Figure 9. Simulated XPS (*a*) and UPS (*b*) spectra of the GdTiGe and GdTiSi compounds (thick solid line) with separated atomic contributions.

Table 4. Chemical shift of the most pronounced photoemission levels for GdTiSi and GdTiGe. The first row shows the binding energies for pure elements. All data are in eV.

Compound	Gd 4f	Ti $2p_{3/2}$	Ti 3p	Si 2s	Si $2p_{3/2}$	Ge 3d	Ge $3p_{3/2}$
	8.1	453.9	33.6	150.2	99.0	29.5	121.7
GdTiSi	0.0	0.0	−0.6	−0.3	−0.6	—	—
GdTiGe	0.5	0.0	−0.3	—	—	−0.7	−0.8

The analysis of the core levels from various elements gives information about the chemical shift which originates from the changes of the potential related to the formation of a compound. As a result, the binding energies of electronic levels are different in compounds and in pure elements. Table 4 shows the chemical shifts of the most pronounced photoemission lines. For Gd only one line is given because for other core levels complex multiplets are formed. For GdTiSi there is no shift of the Gd 4f level and a negative shift for the Si lines, whereas Ti shows different values for a shallow 3p and deeper 2p levels. Negative shift on the Si site may be related to some charge transfer towards these atoms. The situation is similar in GdTiGe but the positive shift at Gd site may mean that some charge has been transferred mainly from the Gd atom. A similar effect was observed in other Gd-Si-Ge compounds [13, 14]. These results are in agreement with the calculations with respect to the total number of electrons which can be ascribed to particular atoms (table 3). In GdTiGe the number of electrons of Gd is lower than in GdTiSi but for Ge it is higher than for Si. This effect may be related to the chemical shifts which indicate more charge transfer from Gd to Ge than to Si.

4. Conclusions

Polycrystalline samples of GdTiGe and GdTiSi were synthesized and their crystal structures were determined. GdTiSi crystallizes in the tetragonal CeFeSi type of structure (P4/nmm) compared with GdTiGe in the tetragonal CeScSi type (I4/mmm). Both compounds exhibit ferromagnetic ordering and the temperature of the transition is very high, such as for a rare-earth compound with non-magnetic metals. It may be a material for future applications. The electronic structure determined from photoemission spectra is in good agreement with the calculations performed with the TB-LMTO method. A particularly interesting result is the exchange splitting of the d bands in Ti and Gd which leads to a relatively large polarization of these hybridized bands in the GdTiGe and antiparallel polarization of the d-states of Ti in the GdTiSi compound. In GdTiGe the polarization of the d-bands is probably a main source of the high magnetic ordering temperature due to the indirect exchange via the d band. The density of s states at the Fermi level is very low and the RKKY interaction seems to play a minor role in the strong ferromagnetic interaction. The calculations indicate also that occupancy of the Gd d band is almost 2 whereas for Ti it is more than 2.5, so it is much greater than has been reported for pure elements. This means that some conversion from the s and p states may take place when the compounds are formed.

Acknowledgements

Support by Polish Committee for Research (grant 2 P03B 129 14) is gratefully acknowledged.

References

[1] Welter R, Morozkin A V, Klosek V, Verniere A and Malaman B 2000 *J. Alloys Comp.* **207** 307
[2] Morozkin A V, Viting L M, Sviridov I A and Tskhadadze I A 2000 *J. Alloys Comp.* **297** 168
[3] Nikitin S A, Tskhadadze I A, Teelgina I V, Morozkin A V and Seropegin Yu D 1998 *J. Magn. Magn. Mater.* **182** 357
[4] Welter R, Verniere A, Venturini G and Malaman B 1999 *J. Alloys Comp.* **283** 54
[5] Morozkin A V 1999 *J. Alloys Comp.* **287** 185
[6] Kido H, Hoshikawa T, Koizumi M and Shimada M 1984 *J. Less Common Metals* **99** 151
[7] Morozkin A V 1999 *J. Alloys Comp.* **284** L7
[8] Morozkin A V 1999 *J. Alloys Comp.* **292** 162–5
[9] Andersen O K and Jepsen O 1984 *Phys. Rev. Lett.* **53** 2571
Andersen O K, Jepsen O and Glötzel D 1985 *Highlights of Condensed Matter Theory* ed F Bassani, F Fumi and M P Tosi (Amsterdam: North-Holland) p 59
Jepsen O and Andersen O K 1971 *Solid State Commun.* **9** 1763
[10] Deniszczyk J and Borgiel W 1997 *J. Phys.: Condens. Matter* **9** 2187
[11] von Barth V and Hedin L 1972 *J. Phys. C: Solid State Phys.* **5** 1629
[12] Langreth D C and Mehl M J 1981 *Phys. Rev.* B **28** 1809
Hu C D and Langreth D C 1985 *Phys. Scr.* **32** 391
[13] Szade J 1997 *J. Magn. Magn. Mater.* **170** 228
[14] Szade J and Skorek G 1999 *J. Magn. Magn. Mater.* **196–197** 699
[15] Szade J and Neumann M 1999 *J. Phys.: Condens. Matter* **11** 3887
[16] Anisimov V I, Zaanen and Andersen O K 1991 *Phys. Rev.* B **44** 943
Anisimov V I, Aryasetiawan F and Liechtenstein A I 1997 *J. Phys.: Condens. Mater* **9** 767
[17] Perdew J P and Zunger A 1981 *Phys. Rev.* B **23** 5048
Svane A 1995 *Phys. Rev.* B **51** 7924
[18] Temmerman W M, Svane A, Szotek Z, Winter H and Beiden S V 2000 *Electronic Structure and Physical Properties of Solids. The Uses of the LMTO Method* ed H Dreysse (Berlin: Springer) p 286
[19] Yeh J and Lindau I 1985 *At. Data Nucl. Data Tables* **32** 1
[20] Brooks M S S, Nordström L and Johansson B 1991 *J. Phys.: Condens. Matter* **3** 2357